SANDIA REPORT
SAND2007-0238
Unlimited Release
Printed January 2007

Edge Energies and Shapes of Nanoprecipitates

John C. Hamilton

Prepared by
Sandia National Laboratories
Albuquerque, New Mexico 87185 and Livermore, California 94550

Sandia is a multiprogram laboratory operated by Sandia Corporation,
a Lockheed Martin Company, for the United States Department of Energy's
National Nuclear Security Administration under Contract DE-AC04-94AL85000.

Sandia National Laboratories

Issued by Sandia National Laboratories, operated for the United States Department of Energy by Sandia Corporation.

Available to DOE and DOE contractors from
U.S. Department of Energy
Office of Scientific and Technical Information
P.O. Box 62
Oak Ridge, TN 37831

Telephone: (865) 576-8401
Facsimile: (865) 576-5728
E-Mail: reports@adonis.osti.gov
Online ordering: http://www.osti.gov/bridge

Available to the public from
U.S. Department of Commerce
National Technical Information Service
5285 Port Royal Rd.
Springfield, VA 22161

Telephone: (800) 553-6847
Facsimile: (703) 605-6900
E-Mail: orders@ntis.fedworld.gov
Online order: http://www.ntis.gov/help/ordermethods.asp?loc=7-4-0#online

SAND2007-0238
Unlimited Release
Printed January 2007

Edge Energies and Shapes of Nanoprecipitates

John C. Hamilton
Micro & Interfacial Sciences
Sandia National Laboratories
Livermore, CA 94551

Abstract

In this report we present a model to explain the size-dependent shapes of lead nano-precipitates in aluminum. Size-dependent shape transitions, frequently observed at nanolength scales, are commonly attributed to edge energy effects. This report resolves an ambiguity in the definition and calculation of edge energies and presents an atomistic calculation of edge energies for free clusters. We also present a theory for size-dependent shapes of Pb nanoprecipitates in Al, introducing the concept of "magic-shapes" defined as precipitate shapes having near zero elastic strains when inserted into similarly shaped voids in the Al matrix. An algorithm for constructing a complete set of magic-shapes is presented. The experimentally observations are explained by elastic strain energies and interfacial energies; edge energies play a negligible role. We replicate the experimental observations by selecting precipitates having magic-shapes and interfacial energies less than a cutoff value.

This Page Intentionally Left Blank.

CONTENTS

FIGURES

TABLES

This Page Intentionally left Blank.

Introduction

This report describes Sandia work aimed at the understanding of nano-precipitate shapes in aluminum. In particular we were motivated by the need to explain size dependent changes in the shape of nano-precipitates observed at sizes less than about 20 nm. Till this work, the proposed explanation for size dependent shape changes was the presumed increased role of edge energies at nano-sizes. In the absence of quantitative calculations of edge energies, it was impossible to verify this theory.

Chapter 1 of this report describes our world first atomistic calculation of edge energies for free clusters, in this case Pd. It presents the new result that edge energies cannot be defined or calculated without a precise definition of edge lengths (and surface areas). In order to define edge lengths and surfaces, we found the concept of the Gibbs dividing surface helpful. In particular we found that using Gibbs equimolar dividing surfaces allowed a precise definition of edge lengths and surface areas, thereby enabling atomistic calculations of edge energies. For the case of free Pd clusters we showed that the edge energy has NO effect on the equilibrium shape of the cluster.

In Chapter 2 we determine the origin of size dependent shape changes for Pb in Al. We first show that atomistic calculations of the total energy are well described by an analytical model which does not include edge energies. We conclude that the precipitate shapes must be determined only by the remaining terms in the analytical model, elastic strain energy and interface energy. Since interface energy alone leads to the Wulff construction and to a size interdependent precipitate shape, the explanation must be dominated by the elastic strain energy. This leads to the concept of "magic-shapes" having nearly zero strain and build from a single sized units of square pyramids and tetrahedra. By selecting magic shapes with relatively low interface energies, the size dependent shape changes and all other experimental observations are well explained.

2a. Edge Energies

A major goal of nano-science is to control the properties of functional nano-structures, including, for example, catalyst particles, quantum dots on surfaces, and inclusions in alloys. Synthesis at the nano-scale is most commonly achieved by controlled self-assembly: understanding the energetic factors governing self-assembly is a critical goal. At the nano-scale, edge energy is commonly invoked as an important driver for self-assembly. For example, edge energies are included in theories for the shapes of snow crystals[1], discussions of surface faceting[2], theories for the shapes of strained Ge pyramids grown on a surface[3], and discussions of Pb inclusions in bulk Al.[4]

Generally edge energies are discussed as an important contributor to the total energy at the nano-scale, yet there appear to be no first-principles or semi-empirical calculations of edge energies.[2] There are two papers which discuss edge energies in terms of broken bond models.[5,6] Other papers treat edge energies as an independent variable, and discuss nano-shapes as a function of the edge energy.[3,7]

Experiments often show changes in the shape of nano-objects as a function of their size. This has been an area of considerable recent interest resulting in a number of experimental[8,9] and theoretical investigations.[10,11,12] Shape transitions are commonly attributed to edge energy effects. Testing these theories requires calculation of quantitative edge energies from an atomistic model to serve as input for continuum calculations of shape transitions. While one might suppose that atomistic calculation of edge energies would be routine, I show that there is an ambiguity in the atomistic definition of edge energies, and discuss a resolution of this ambiguity.

The problem in defining edge energies is related to the problem of defining the exact position of an atomic surface in the direction normal to the surface. This problem is addressed by the well-known concept of the Gibbs dividing surface. As Gibbs points out, "It will be observed that the position of this surface is as yet to a certain extent arbitrary"[13]. Depending on the exact position chosen for the Gibbs dividing surface, the surface contribution to extensive

properties of the solid will vary. For a single component system, a common choice of dividing surface is the equimolar surface.[14] The equimolar surface is defined so that the surface contribution to the molar amount of the solid is zero. Finally, we note that Gibbs has mentioned the possibility of calculating line properties such as tension at the linear intersection between two or more dividing surfaces. To quote Gibbs, "We may here remark that a nearer approximation in the theory of equilibrium and stability might be attained by taking special account, ..., of the lines in which surfaces of discontinuity meet. .....We might recognize linear densities of energy, of entropy, and of the several substances which occur about the line."[15] In this paper I describe the application of such an approach to determine the linear density of energy at an edge formed by the intersection of two dividing surfaces.

In this paper we will assume that the clusters we are dealing with can be represented by flat surfaces (facets) that intersect forming straight edges. Given this assumption, the total energy of a polyhedral cluster, with shape independent of edge length, can be written in the form:

$$E_{total} = As^3 + Bs^2 + Cs + D \qquad (1).$$

where s is the edge length and A, B, C, and D are coefficients related to the bulk, surface, edge and vertex energy respectively. Theories for equilibrium shape, including the Wulff construction, are based on this assumption of flat facets with an orientation dependent surface energy.

The purpose of this section is to demonstrate the extremely large uncertainties that can result from the failure to rigorously define edge length. We include this section, because implicit assumptions are often made in the definition of edge energies. Hopefully the reader will be convinced that this is more than a minor semantic problem, and will be inoculated against erroneous assumptions which may occur in more abstract discussions of the subject. The reader may chose to read this section quickly, continue to section III which proposes a precise definition of edge length based on equimolar dividing surfaces, and return to this section as desired.

We illustrate the problem by considering quantitative calculations for a cuboctahedral cluster. Consider such a cluster having n atoms along each edge as shown in Figure 1.

First we calculate the total energy, $E_{total}(n)$, of the cluster using an embedded atom method (EAM) calculation. Table 1 gives $E_{total}(n)$ and the total number of atoms, N, for Pd clusters with $5 \leq n \leq 9$.

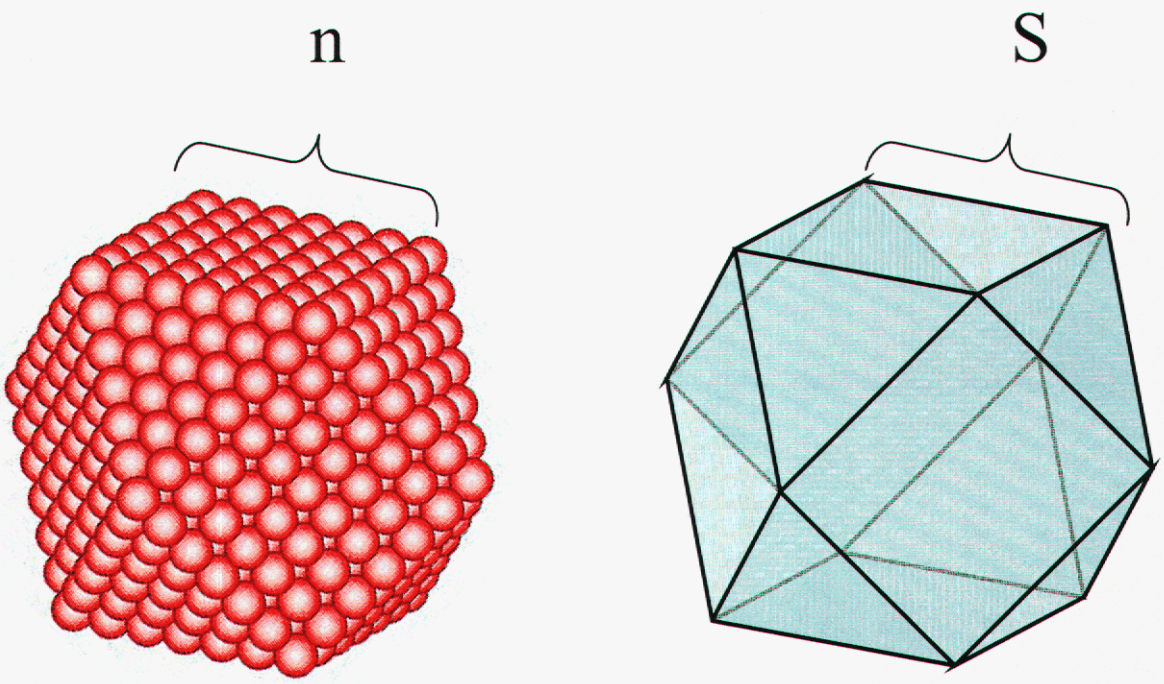

Figure 1. A cuboctahedral cluster of Pd atoms having n=7 atoms along each edge is shown on the left. A geometrical cuboctahedron having edge lengths, s, is shown on the right. Theories such as the Wulff construction, which predict shapes as a function of surface and edge energies, implicitly assume that the surfaces are flat, and that the edges are straight intersections of these surfaces. The major point of this paper is that defining and calculating edge energies requires a precise definition of s as a function of n. In section III this function is derived based on the choice of the geometrical surfaces as equimolar Gibbs dividing surfaces.

The next step is to expand the total energy in powers of the edge length, s, as in equation (1) above. From the coefficients A, B, C, and D, the bulk, surface, edge and vertex energies respectively can be calculated. The problem is that to determine these coefficients, a precise definition for the edge length, s, measured in Å, as a function of n is essential. The correct

way to do this is not obvious, although it seems reasonable that the correct value would lie somewhere in the range

$$(n-1)d \le s \le nd \qquad (2)$$

where a is the fcc lattice constant and $d=a/\sqrt{2}$ is the nearest neighbor distance. In order to see how critically important this is, we will consider three possible choices for s, namely s=(n-1)d, s ≈ (n - ½)d, and s=nd. (The exact definition of the intermediate choice will be given by equation 5 appearing later in this paper). Figure 2a shows a plot of $E_{total}(s)$ for these three definitions of s.

Table 1. Results of embedded atom method calculation of energies of Pd cuboctahedral clusters. The number n is the number of atoms on the edge of the cuboctahedral cluster (see figure 1). The number N is the total number of atoms in the cluster. E_{total} is the total energy of the Pd cluster from an EAM calculation. Since the atomic positions were relaxed in the total energy calculation, changes of the total energy due to relaxation of surface and edge atom positions are included in the total energy. The last column shows the total energy after subtracting the bulk energy, NE_{coh}.

n number of atoms on edge	N total number of atoms	E_{total} (eV)	E_{total}-NE_{coh} (eV)
5	309	-1086.234	121.956
6	561	-2012.793	180.717
7	923	-3357.798	251.132
8	1415	-5199.442	333.208
9	2057	-7615.919	426.951

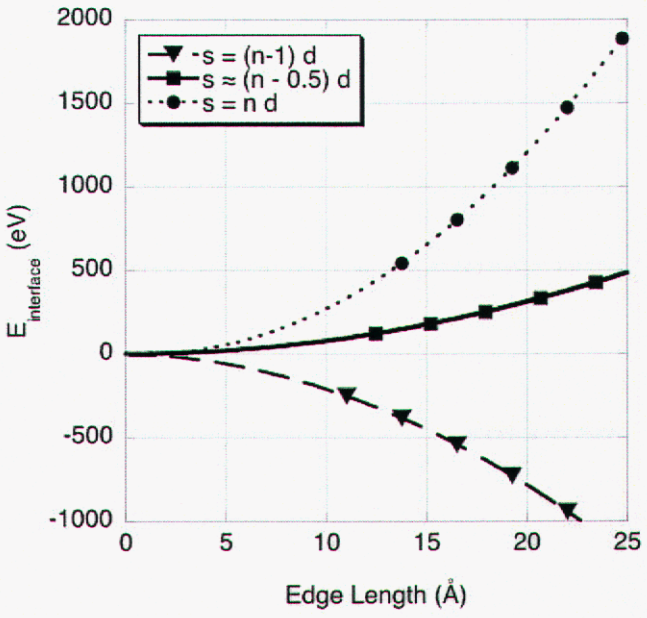

Figure 2a. This figure shows the importance of a precise definition of the edge length, s=f(n), as a function of the number of atoms, n, along an edge. The first graph (2a) plots the calculated total energy as a function of the edge length for three different definitions of s. The curves labeled "s=(n-1)d" and "s=nd" represent the limiting definitions (d is the nearest neighbor distance, see equation 2 of the text). The curve labeled "s ≈(n-0.5)d" is actually plotted using equation 5 of the text to define edge length. Least squares fitting to a cubic polynomial (equation 1) gives a term As^3, the bulk contribution to the total energy.

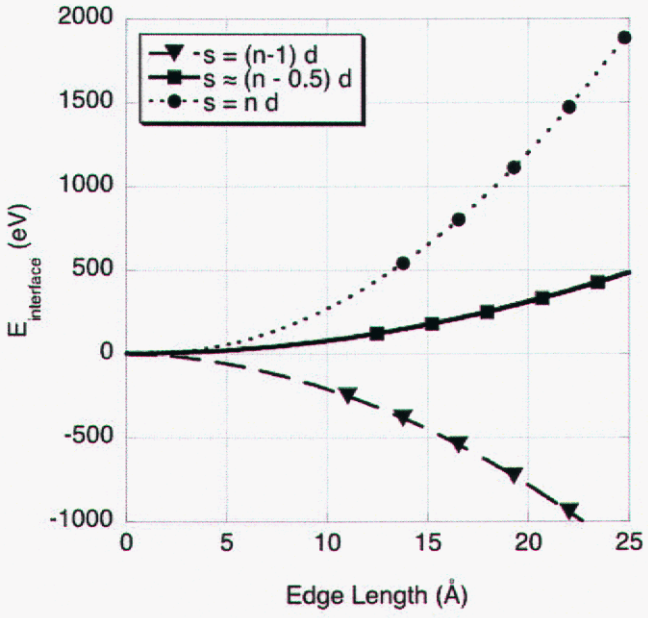

Figure 2b. The second graph (2b) plots the interface energy, defined as Etotal-As3, for the three definitions of s. We will show in section IV that the value of the interface energy is reasonable for " s ≈(n-0.5)d". The other definitions give interface energies which are much too large and/or incorrect in sign.

For all three definitions least square fitting gives the same bulk energy coefficient, A=-0.62621eV/Å^3. The total interface energy is calculated as:

$$E_{interface} = Bs^2 + Cs + D = E_{total} - As^3 \qquad (3)$$

Figure 2b shows a plot of $E_{interface}(s)$ for the three different definitions of s. Only one of these curves gives a surface energy anywhere near the correct value. As we shall latter verify, the correct value is given by the curve labeled s ≈ (n - ½)d. The curve for s=nd gives surface energies that are approximately four times the correct value! The curve for s=(n-1)d gives surface energies that are approximately two times the correct value and have the wrong sign!

This shows that the problem of defining the edge length will be crucial to the definition and calculation of edge energies.

An alternate approach is to begin by subtracting the total bulk cohesive energy, NE_{coh}, from E_{total} to isolate the interface terms. Here N is the total number of atoms in the cluster and E_{coh} is the bulk cohesive energy per atom. This approach is standard in slab calculations for surface energies. We show here that it doesn't solve the problem of defining the edge length or allowing calculation of edge energies.

We start with the calculation of E_{total} using the embedded atom method and subtract the bulk energy, NE_{coh}, from the total energy. Table 1 of the text gives numerical values for E_{total}-NE_{coh} for cuboctahedral clusters having 5 to 9 atoms on an edge. Since E_{total}-NE_{coh} is the sum of the surface, edge and vertex energies, it can be written as a quadratic polynomial of the edge length, s.

$$E_{total}-NE_{coh} = Bs^2+Cs+D \qquad (4)$$

As before, we must define s before we can fit a polynomial. We consider the same definitions of s used previously, s=(n-1)d, s ≈ (n - ½)d, and s=nd. Figure 3a shows a plot of E_{total}-NE_{coh} plotted using these three definitions for s. These functions are fit by a quadratic polynomial as in equation (4). For these three definitions of s, the fitting coefficient B is equal to 0.77061. From the cubic fit we can also plot the sum of the edge and vertex, $E_{edge}+E_{vertex}=Cs+D$, as shown in figure 3b. The edge energy would be $\varepsilon=C/24$ and would be proportional to the slope seen in the plot. Since the slope of the three lines is very different depending on the definition of s, the edge energy cannot be calculated without a precise definition for the edge length.

The problem of defining edge lengths is related to the problem of defining the exact position of the surface of a solid. The well-known concept of the Gibbs dividing surface is a rigorous solution to the problem. We can place the Gibbs dividing surface where we like (within reason), but the value of surface excess quantities will depend on the position of the dividing surface. In order to define edge lengths, we consider a faceted cluster as being built from intersecting dividing surfaces, one surface for each facet. The edges are formed by the

intersection of two dividing surfaces and the vertices are formed by the intersection of three dividing surfaces. For the case of a cuboctahedron, figure 1 shows the atomic cluster on the left and the geometrical shape formed from the assemblage of dividing surfaces on the right. Defining the edge length, s, is thus seen to be a problem in choosing the position of the dividing surfaces.

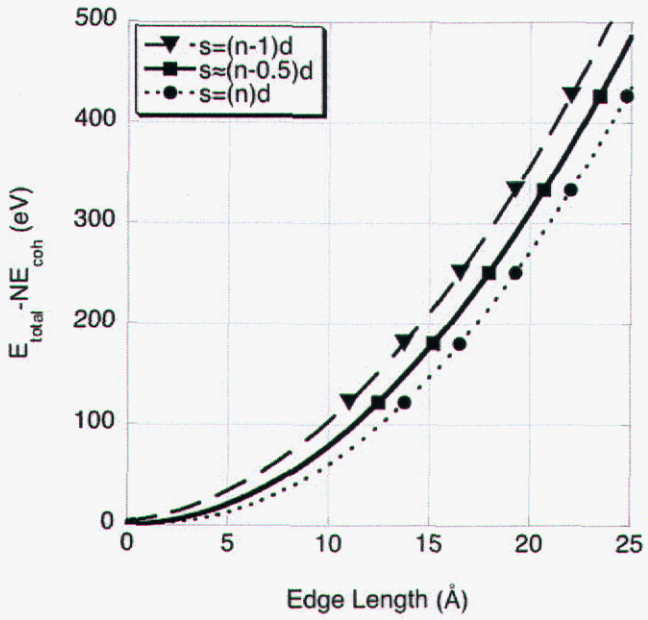

Figure 3a. Figure 3a plots the quantity, Etotal-NEcoh, for three plausible definitions of the edge length, s, defined in the text and in the caption for figure 2. Least squares fitting to a quadratic polynomial (equation 4) gives a term Bs^2, the surface contribution to the total energy.

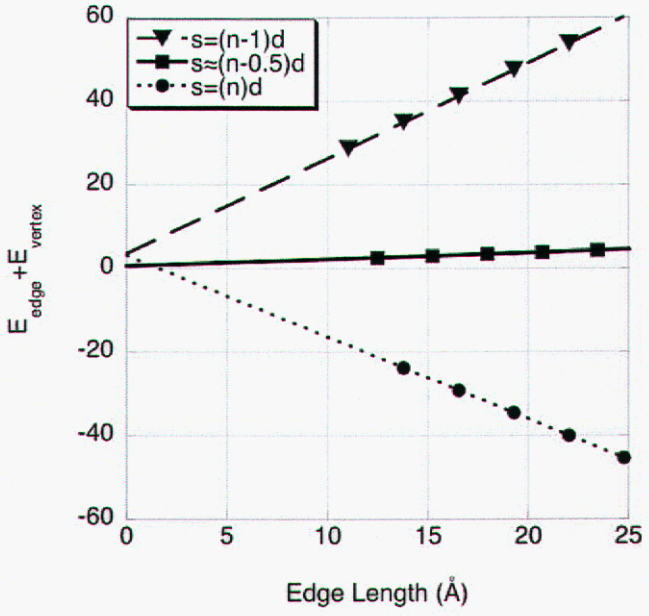

Figure 3b. The second graph (3b) plots the sum of the edge and vertex energy, defined as Etotal-NEcoh-Bs2, for the three definitions of s. The calculated edge energy would be proportional to the slope of the lines. The three different definitions of s give vastly different results for the edge energy. This demonstrates again that a rigorous and precise definition of the edge length, s, is essential in order to define and/or calculate the edge energy.

While the position of a dividing surface is generally arbitrary, we will find that the problems described in the previous section are resolved in a consistent manner by defining the edge length using equimolar dividing surfaces. To see this, we refer to equation 1. We know that the total bulk energy, As^3, should equal NE_{coh}, where E_{coh} is the bulk cohesive energy per atom and N is the total number of atoms. For a cuboctahedron formed by dividing surfaces, the definition of a dividing surface implies that the total bulk energy is equal to the constant energy density of bulk palladium, $\rho = \frac{4E_{coh}}{a^3}$, integrated over the volume of the cuboctahedron formed by the dividing surfaces, $V = \frac{5\sqrt{2}}{3}s^3$. The bulk energy of the

cuboctahedron formed by the dividing surfaces is Vρ. The total number of atoms in a cuboctahedral cluster is $N = \frac{10n^3}{3} - 5n^2 + \frac{11n}{3} - 1$. Substituting these equations for N,V, and ρ in the equation $NE_{coh}=V\rho$ and solving for s we find:

$$s = \left[\sqrt[3]{n^3 - \frac{3n^2}{2} + \frac{11n}{10} - \frac{3}{10}}\right]\left(\frac{a}{\sqrt{2}}\right) \qquad (5)$$

This gives us a precise definition of s, as needed to separate bulk, surface, edge and vertex energies. It is will also be convenient to have a series expansion for s. Expanding equation 5 in a Taylor series gives:

$$s = \left[n - \frac{1}{2} + \frac{7}{60n} + O\left[\frac{1}{n^2}\right]\right]\left(\frac{a}{\sqrt{2}}\right) \qquad (6)$$

Since we are ultimately interested in calculating energies, this derivation was based on energy density. A derivation using number density would be nearly identical, and the final definition of s would be the same. This means that the dividing surfaces we will use to define s are equimolar surfaces.

With this definition for s, we can return to the problem of calculating surface, edge, and vertex energies for the cuboctahedron. We plot $E_{total}(s)$ with s defined by equation (5). This is the curve labeled "$s \approx (n - ½)d$" in figure 2.

From a cubic fit (equation 1) we get the coefficients A, B, C, and D which relate directly to the bulk (cohesive) energy, the surface energy, the edge energy and the vertex energy. The log-log plot shown in figure 4, plots $-As^3$, Bs^2, Cs, and D. We will now consider each term in order to verify that the bulk and surface energies agree with standard EAM calculations, and to obtain numerical values for the edge and vertex energies.

We consider first the bulk energy term. The cluster least square fit gives A=-0.62621 eV/Å^3. The volume of the cuboctahedron is $V = \frac{5\sqrt{2}}{3}s^3$ and the energy density of bulk Pd is $\rho = \frac{4E_{coh}}{a^3}$. The EAM functions used were fitted to give E_{coh}=3.91eV and

a=3.89Å. Thus the predicted value of A is $-\frac{V\rho}{s^3} = -0.62626\ \text{eV}/\text{Å}^3$ in good agreement with the EAM cluster least square fit.

Next we consider the surface energy term. The least square fit gives B=0.76818 eV/Å^2. The (111) surface area of the cuboctahedron is $A_{111} = (2\sqrt{3})s^2$ and the (100) surface area of the cuboctahedron is $A_{100} = 6s^2$. The EAM functions used here give surface energies of $\gamma_{111} = 75.82\text{meV}/\text{Å}^2$ and $\gamma_{100} = 85.15\text{meV}/\text{Å}^2$ from bulk slab calculations. Thus the predicted value of B is $\frac{A_{100}\gamma_{100} + A_{111}\gamma_{111}}{s^2} = 0.7735\ \text{eV}/\text{Å}^2$ in good agreement with the EAM cluster least square fit.

Finally we are ready to calculate the edge energy of a cuboctahedron. Because all of the edges are formed by the intersection of a (111) surface and a (100) surface, we will use the notation, $\varepsilon_{111\text{-}100}$ to denote the edge energy. The cluster least square fit gives C=0.20706 eV/Å.

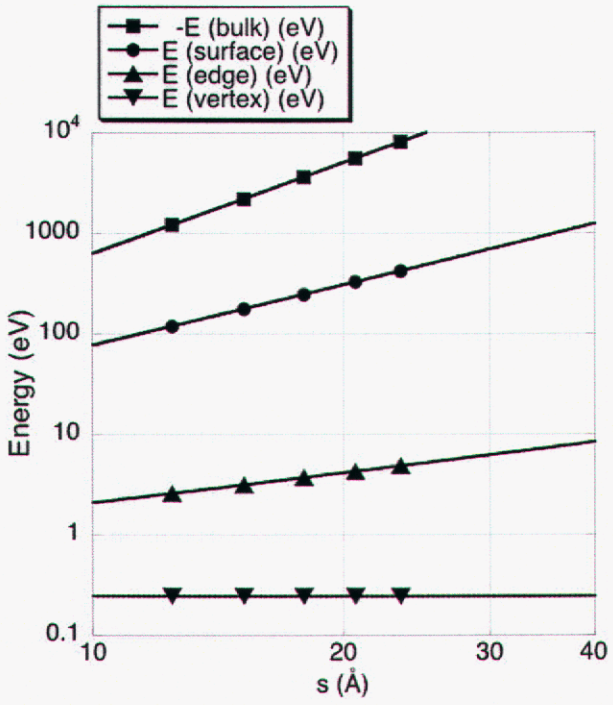

Figure 4. This figure shows the values of the bulk, surface, edge, and vertex energies from EAM calculations for Pd cuboctahedral clusters having $5 \le n \le 9$ atoms on an edge. The edge length, s, was defined by the equimolar surfaces (see equation 5 of the text). The total energy was fit by a cubic polynomial (see equation 1 of the text). The bulk, surface, edge and vertex contributions are plotted here as $-As^3$, Bs^2, Cs, and D respectively. The negative of the bulk energy is plotted so that all four energies can be compared on a single log-log plot.

The total edge length of the cuboctahedron is 24s. Consequently we calculate $\varepsilon_{111\text{-}100}=C/24=8.63\text{meV/Å}$. This calculated value for the edge energy is included in Table 2.

The last step is to calculate the vertex energy of the cuboctahedron. The cuboctahedron has 12 vertices at which two (111) facets meet two (100) facets.

The cluster least square fit gives D=0.24441eV. Dividing by 12 we get the vertex energy, $\alpha_{cuboct}=20.3\text{meV}$.

The definition of edge length, s, for an octahedron follows the procedure described for a cuboctahedron in section III. Here it will suffice to give the equations which define the edge length based on equimolar dividing surfaces. We find:

$$s = \left[\sqrt[3]{n^3 + \frac{n}{2}}\right]\frac{a}{\sqrt{2}} \qquad (7) \quad \text{and}$$

Table 2. This table gives the edge energies calculated from EAM calculations and from a bond-breaking model described in the appendix.

	$\varepsilon_{111\text{-}111}$	$\varepsilon_{111\text{-}100}$
EAM	4.6 meV/Å	8.6 meV/Å
Bond-breaking	0.0 meV/Å	0.0 meV/Å

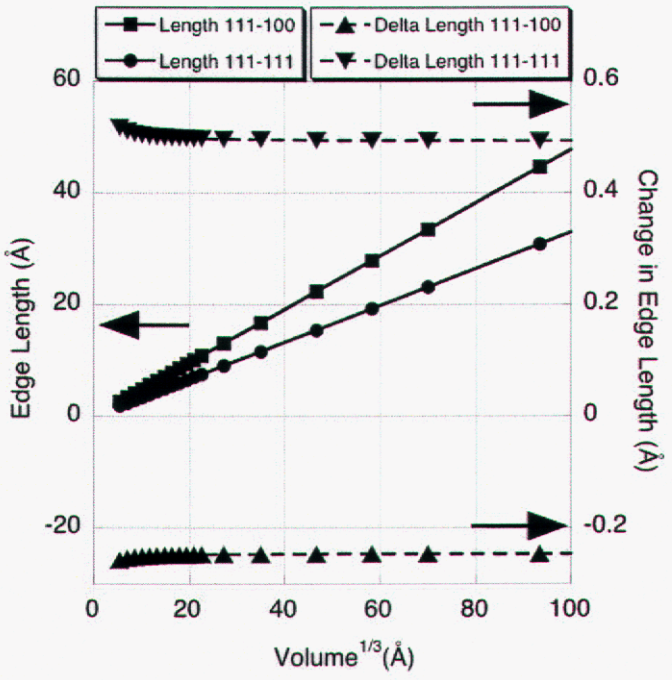

Figure 5. This plot shows the results of a Wulff construction (minimizing the surface energy of an atomic cluster, subject to the constraint of constant volume). The values for surface energy are taken from the calculations in the text. The left vertical axis shows the edge lengths predicted by the Wulff construction as a function of the cube root of the cluster volume. The plot also shows the changes in the edge lengths predicted by including the edge energies given in table 2 to the total energy (see equation 9 of the text) Since the changes in edge length are <0.6Å for all cluster sizes, and edge lengths are constrained by discrete atomic distances, the edge energies will have essentially no effect on the shape of Pd clusters at any length scale.

$$s = \left[n + \frac{1}{6n} + O\left[\frac{1}{n^3}\right] \right] \frac{a}{\sqrt{2}} \qquad (8)$$

For an octahedron the edge length defined by equation 7 is approximately nd, whereas for a cuboctahedron the edge length defined by equation 5 is approximately (n - ½)d. The fact that the definition of s is so different for these two cases emphasizes the importance of a rigorous and precise definition. The process for fitting the total energy of the octahedron with a bulk, surface, edge and vertex term is done much as for the cuboctahedron. The bulk and surface

energies from the series expansion for the total energy of the octahedron are in good agreement with values from conventional EAM calculations. The edges of the octahedron are formed at the intersection of two (111) facets. Thus we will use the notation $\varepsilon_{111\text{-}111}$ for the edge energy. We calculate $\varepsilon_{111\text{-}111} = 4.60\text{meV}/\text{Å}$ and α_{oct}=127meV. Table 2 of this paper summarizes the values of the edge energies found from these EAM calculations and gives the values of the edge energies from a bond-breaking model described in the appendix.

One of the major motivations for calculating edge energies (see section I) was to examine the possible role of edge energies in causing shape transitions for nanoparticles. For larger clusters the equilibrium shape of a particle is governed primarily by the surface energies and the lowest energy shape is determined by the Wulff construction. As an example, consider a truncated octahedral particle. We will assume here that the surface energy of surfaces other than (100) and (111) are sufficiently large, and thus that they are not part of the equilibrium shape. The Wulff shape is determined by minimizing the interface energy, $E_{\text{interface}} = 6A_{111}\gamma_{111} + 8A_{100}\gamma_{100}$, subject to the constraint of constant volume. Here A_{111} is the area of a (111) facet and A_{100} of is the area of a (100) facet. We will use the notation $L_{111\text{-}111}$ for the edge length at the intersection of two (111) facets and $L_{111\text{-}100}$ for the edge length at the intersection of a (100) and a (111) facet. Figure 4 shows these two edge lengths as a function of the cube root of the particle volume, a convenient measure of particle size.

By adding edge energies to the interface energy we can determine their effect on cluster shape. The interface energy becomes

$$E_{\text{interface}} = 6A_{111}\gamma_{111} + 8A_{100}\gamma_{100} + 12L_{111\text{-}111}\varepsilon_{111\text{-}111} + 24L_{111\text{-}100}\varepsilon_{111\text{-}100}. \quad (9)$$

By minimizing the interface energy subject to the constraint of constant volume the edge lengths can be determined. Since $\varepsilon_{111\text{-}111}$ is smaller than $\varepsilon_{111\text{-}100}$ the effect of the edge energies will be to lengthen $L_{111\text{-}111}$ and shorten $L_{111\text{-}100}$, while keeping the total volume constant. Figure 4 shows the changes in the edge lengths which result from including edge energies. $L_{111\text{-}111}$ is increased by about 0.5Å and $L_{111\text{-}100}$ is decreased by about 0.25Å over the whole range of cluster size. Since these changes are much less than the nearest neighbor distance, the actual cluster shape will rarely be changed by the edge energies for any cluster size.

The basic result of this paper is that edge energies cannot be defined or calculated without careful and precise definitions for edge lengths and facet areas. A precise definition is suggested based on the concept of intersecting equimolar surfaces. Using this definition, the edge and vertex energies have been calculated for Pd clusters. Finally, I show that the calculated edge energies will have essentially no effect on the equilibrium crystal shape for Pd nano-clusters. The issues raised here will be crucial for future work on the role of edge energy in self-assembly of nanostructures. They also demonstrate the challenges to be encountered in applying continuum concepts at the nano-scale.

This Page Intentionally Left Blank.

2b. Bond Breaking Model of Edge Energy

Previous discussions of edge-energies have commonly used bond-breaking models.[5,6] At the atomic level, every atom can easily be classified as a bulk, surface, edge, or vertex atom. Even though every atom can be classified, the correct definition of edge length and surface area remains ambiguous. From the atomic point of view, the ambiguity is that "edge atoms" could equally well be considered as being part of the areas of the two surfaces meeting to form the edge.

In order to make contact with the previous work, it is appropriate to revisit the bond-breaking model and to calculate the edge and vertex energies for fcc clusters using the definition of surface area and edge length based on intersecting equimolar dividing surfaces. In this appendix only, the length unit used is the nearest neighbor distance and the energy unit used is one-half of the energy required to break a nearest neighbor bond. In these energy units, the bulk cohesive energy is 12, and the surface energies (for an infinite planar surface) are $\gamma_{111} = 2\sqrt{3}$ and $\gamma_{100} = 4$. In order to distinguish between the octahedron and the cuboctahedron, we will use subscripts. For example, the number of atoms on an edge will be written n_{oct} for the octahedron and n_{cuboct} for the cuboctahedron.

The calculation parallels the EAM calculations described in the body of this paper. However, because we can readily calculate the total interface energy by counting broken bonds, there is no need to include bulk terms in the derivation. Thus the total interface energy is written in powers of the edge length, as $E_{interface} = Bs^2 + Cs + D$.

In order to calculate the interface energy for an octahedron, with n_{oct} atoms on an edge, it is necessary to count the total number of broken bonds. For an octahedral cluster there are $4(n_{oct} - 3)(n_{oct} - 2)$ surface atoms each having 3 broken bonds, $12(n_{oct} - 2)$ edge atoms each having 5 broken bonds, and 6 vertex atoms each having 8 broken bonds. Summing all these contributions, the total number of broken bonds at the surface, edge and vertex atoms is $E_{interface} = 12n_{oct}^2$.

At this point we equate the two expressions for the interface energy and write:

$$Bs_{oct}^2 + Cs_{oct} + D = 12n_{oct}^2 \qquad (9)$$

Next we use the definition for the edge length, s_{oct}, given by equation (8). We substitute $s_{oct}=n_{oct}+1/n_{oct}$ in equation (9), collect equal powers in n_{oct}, and discard all terms with negative powers of n_{oct}. By equating coefficients of terms having the same power in n_{oct}, we find B=12, C=0, and D=-4. Since $Bs_{oct}^2 = \text{Area}_{oct}\gamma_{111}$ and $\text{Area}_{oct} = 2\sqrt{3}s_{oct}^2$ we find $\gamma_{111} = 2\sqrt{3}$ from our cluster calculation in perfect agreement with the infinite plane value.

Since $C = 12\varepsilon_{111\text{-}111}$ we find that the edge energy, $\varepsilon_{111\text{-}111}$, for the octahedron is identically zero in a broken bond model. Since $D = 6\alpha_{vertex}$, we find the vertex energy for the octahedron to be $\alpha_{vertex} = -2/3$ for the octahedral cluster.

The calculation for a cuboctahedron is similar. For a cuboctahedron there are $4(n_{cuboct}-3)(n_{cuboct}-2)$ (111) surface atoms each having 3 broken bonds, there are $6(n_{cuboct}-2)^2$ (100) surface atoms each having 4 broken bonds, there are $24(n_{cuboct}-2)$ edge atoms each having 5 broken bonds, and there are 12 vertex atoms each having 8 broken bonds. Summing all these contributions, the total number of broken bonds for the cluster is $E_{interface} = 36n_{cuboct}^2 - 36n_{cuboct} + 12$.

As before, we equate the two expressions for the interface energy and write:

$$Bs_{cuboct}^2 + Cs_{cuboct} + D = 36n_{cuboct}^2 - 36n_{cuboct} + 12 \qquad (10)$$

We substitute the definition for s_{cuboct} given by equation (6) into equation (10), collect equal powers of n_{cuboct}, and discard all terms with negative powers of n_{cuboct}.
By equating coefficients to the same order in n_{cuboct}, we find B=36, C=0, and D=-5.4. The value for B corresponds to exactly to the value expected based on the areas and surface energies of the two types of facets. We also find $\varepsilon_{111\text{-}100}=0$ and $\alpha_{vertex}=-0.45$.

The important conclusion from the bond-breaking model is that if edge length and surface area of clusters are defined using equimolar dividing surfaces, the calculated surface energies are equal to their value from infinite slab calculations and the edge energies of the two types of edges are precisely zero. In reference 6, using bond-counting methods, the authors comment: "The main result of our calculations is the surprising agreement of the microscopic results ... with the predictions of the macroscopic Wulff's rule, even for particles as small as those with 2000 or 3000 atoms" (in spite of the fact that ~7% of atoms are edge or vertex atoms). The calculations presented in this appendix show that edge energies are zero for a simple bond-breaking model, thus explaining the previous "surprising" results.

This Page Intentionally Left Blank.

3. Pb Nanoprecipitates in Al: Magic-Shape Effects Due to Elastic Strain

A major goal of nanoscience is to understand and control the properties of functional nanostructures, including, for example, catalyst particles, quantum dots on surfaces, and inclusions in alloys. These properties are often determined by the nanostructure shape, and edge energy is commonly invoked as an important factor in determining shape. For example, edge energies are included in theories for the shapes of snow crystals,[16] discussions of surface faceting,[17] theories for the shapes of strained Ge pyramids grown on a surface,[18] and discussions of Pb inclusions in bulk Al.[19] For larger objects, the Wulff construction, based on minimization of interfacial energy subject to a constraint of constant volume, is well known and well tested. The Wulff construction predicts that the cluster shape will be independent of cluster size. Experimentally, however, changes in cluster shapes are often observed as cluster sizes approach the nanoscale i.e. less than about 20nm across. Generally such size-dependent shape effects are attributed to the increasing contribution of edge energies relative to the interfacial energies at the nanoscale. Until very recently[20,21], no atomistic calculations of edge energies had been published, making it essentially impossible to compare experimental and theoretical work on cluster shapes at the nanoscale.

In the present letter we present a theoretical examination of extensive experimental data on size-dependent shapes of Pb nanoprecipitates in Al.[19,22] First, we present embedded atom method (EAM) calculations of the total precipitate energies for a range of sizes and for three different shapes (octahedral, tetrakaidecahedral, and cuboctahedral, see insert in figure 2). Next, we present an analytical model for the energies of these precipitates. By comparing the EAM calculations with the analytical model, we show that edge energies play little or no role in determining the shapes of these nanoprecipitates and that the experimental results must be explained solely by the minimization of the sum of the interfacial energy and the strain energy. Finally we present an algorithm for generating precipitate shapes with very small strain energies. We use the term, "magic shapes", to describe these special precipitate shapes. The minimization of precipitate interfacial energies subject to the "magic shape" constraint, explains the experimental size-dependent shape effects.

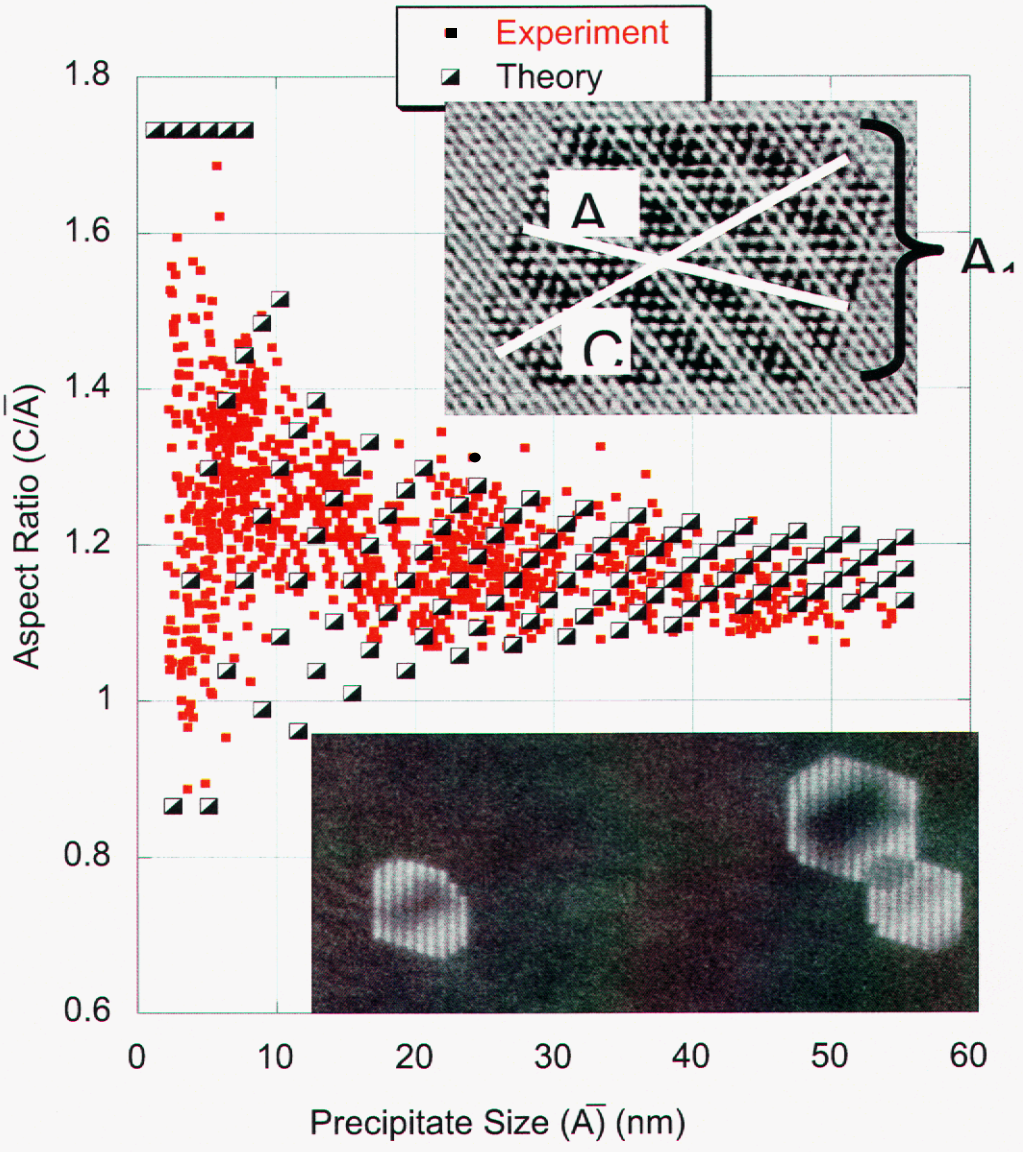

Figure 6. This figure shows aspect ratios as a function of the precipitate size. The red points are experimental data, the black symbols are the prediction of our "magic-shape" theory. Some of the experimentally observed precipitates (examples shown as micrograph inserts) do not exhibit the O_h symmetry predicted by the Wulff construction. Large clusters have aspect ratios, $C/\overline{A} = 2C/(A_1 + A_2)$, very close to the Wulff construction prediction. As the cluster size decreases, the mean aspect ratio increases and the scatter in the aspect ratios increases dramatically. The magic shape theory (black points) represents a complete set of precipitates with O_h symmetry having near-zero elastic strain and energies $\Delta E = E_{precipitate} - E_{Wulff} < 60eV$. The agreement between the "magic shape" theory and experiment is very good.

Figure 6 presents a brief summary of the experimental observations (red points on the plot). These precipitates were formed by Pb ion-implantation followed by annealing.[22] A few of the smaller precipitates are octahedral, bounded by {111} type Pb/Al interfaces. The largest precipitates are approximately tetrakaidecahedral, bounded by {111} and {100} type Pb/Al interfaces, as shown in the insert in figure 6. We denote the spacing between a pair of {100} type facets as C, and the spacing between the pairs of {111} type facets as A_1 and A_2. The mean spacing between the pairs of {111} facets is $\overline{A} = (A_1 + A_2)/2$. The Pb/Al interfacial free energies, γ_{100} and γ_{111}, have previously been calculated as a function of temperature with the embedded atom method (EAM)[23]: $\gamma_{100} = 48.44$ meV/Å^2 and $\gamma_{111} = 41.44$ meV/Å^2 at T=400K (in the vicinity of the annealing temperature). The predicted aspect ratio from the Wulff construction at this temperature is thus $C/A = \gamma_{100}/\gamma_{111} = 1.165$. For larger precipitates, the measured aspect ratio is close to this value; however, as seen in figure 6, smaller precipitates behave quite differently, and exhibit a wide range of aspect ratios. The major goal of this paper is to understand this size-dependent shape effect.

We began with EAM calculations of precipitate energies as a function of size and shape. While a large variety of EAM calculations were performed, here we will discuss only a small subset of the calculations involving homogeneously strained regular polyhedra (octahedra, tetrakaidecahedra, and cuboctahedra). The EAM potentials used were developed by Adams and coworkers.[24] We started the calculation by constructing a rectangular solid of fcc Al with periodic boundary conditions. In the [001] direction the period was ~140Å, in the [110] and $[1\bar{1}0]$ directions the period was ~100Å. Next we removed a regular polyhedron of Al atoms with n atoms on an edge. We will use the notation n_{oct}, n_{tetra}, and n_{cub} for the number of edge atoms on the removed polyhedron for the octahedron, tetrakaidecahedron, and cuboctahedron respectively. Finally we inserted an identically shaped polyhedron of Pb atoms with m_{oct}, m_{tetra}, or m_{cub} atoms on an edge. By removing an Al polydedron and inserting a Pb polyhedron having the same shape, we ensured that the strain would be homogeneous.

Since the lattice constants of Pb and Al are a_{Pb}=4.95Å and a_{Al}=4.05Å respectively, a strain-free octahedral precipitate would have $n_{oct}/m_{oct} = a_{Pb}/a_{Al} = 11/9 = 1.22$. Table 3 lists the

values of n and m which will result in relatively small strains; additional cases were also studied in the range $1.15 \leq n/m \leq 1.33$, thereby placing an upper limit on the strain.

Table 3. This table gives values for n and m that correspond to the low strain precipitates. Octahedra, tetrakaidecahedra, cuboctahedra with m Pb atoms on an edge can be inserted in Al voids made by removing the same shape polyhedra with n Al atoms on an edge. For the cases with tensile and compressive strain, the strain (in percent) is also given.

n-m	(m,n) η Tensile Strain	(m,n) Zero Strain	(m,n), η Compressive Strain
1	(4,5) 2.25%		(5,6) 1.8%
2	(8,10) 2.25%	(9,11)	(10,12) 1.8%
3	(13,16) 0.70%		(14,17) 0.65%
4	(17,21) 1.06%	(18,22)	(19,23) 0.96%
5	(22,27) 0.41%		(23,28) 0.40%
6	(26,32) 0.70%	(27,33)	(28,34) 0.65%

Having created a starting configuration with a Pb polyhedron inserted in similarly shaped Al void, the atomic positions were relaxed using conjugate-gradient minimization of the total energy, E_{total}. Next we subtracted the total cohesive energy of the Pb and Al atoms to calculate the total energy of the precipitate,

$$E_{precipitate}=E_{total}-N_{Al}E_{cohAl}-N_{Pb}E_{cohPb}.$$

Here N_{Al} and N_{Pb} are the total number of Al and Pb atoms in the periodic cell, and E_{cohAl} and E_{cohPb} are the bulk cohesive energies per atom calculated using the EAM potentials. This energy is plotted as a function of $N_{Pb}^{2/3}$ in figure 7a (the interface area for a given shape is proportional to $N_{Pb}^{2/3}$). We will find that the roughly linear dependence of $E_{precipitate}$ on $N_{Pb}^{2/3}$ represents the contribution of the interfacial energy, $E_{interface}$, and that the curvature of the individual lines represents the contribution of the strain energy, E_{strain}. We will also show that the contribution of the edge energy, E_{edge}, is negligible.

To prove these points, we neglect edge energy for the moment and write:

$$E_{precipitate} = E_{interface} + E_{strain}.$$

7a 7b

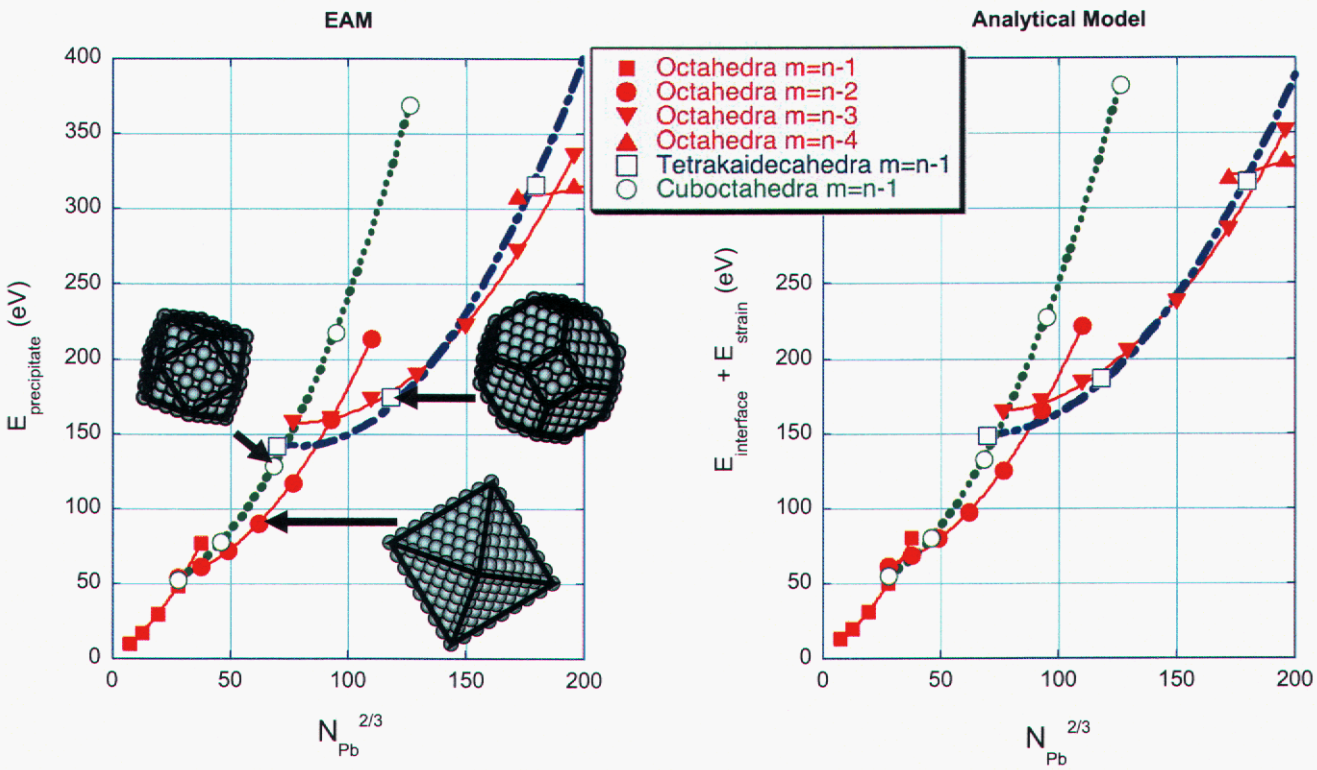

Figure 7a and 7b. Precipitate energies for small Pb inclusions in an Al matrix. Three different shapes are considered, octahedra, tetrakaidecahedra, and cuboctahedra, as seen in the inserts in 7a. The left hand plot shows the precipitate energy at T=0K calculated using EAM. The right hand plot shows the sum of the interface energy and the strain energy calculated using the analytical model discussed in the text. The lines are cubic polynomial fits to the calculated values. The illustrated clusters correspond to $(m_{oct},n_{oct})=(9,11)$, $(m_{trunc},n_{trunc})=(4,5)$, and $(m_{cub},n_{cub})=(5,6)$ for the octahedron, truncated octahedron and cuboctahedron respectively.

Next we present an analytic model for $E_{precipitate}$ assuming homogeneous strain of the precipitate. The interface energy is $E_{interface}= A_{111}\gamma_{111} + A_{100}\gamma_{100}$,where A_{100} and A_{111} are the total areas of the {100} and {111} facets. The energies per unit area of the Pb/Al interface calculated in reference 23 using identical EAM potentials are γ_{111} = 28.33meV/Å^2 and γ_{100} =

37.13meV/Å^2. We use T=0K energies here, because the EAM calculation shown in figure 7a is a 0K calculation.

It would appear straightforward to calculate A_{111} or A_{100} for a polyhedron with m atoms on an edge, but it is not. This is due to a fundamental ambiguity in the definition of edge lengths and interface areas for atomic systems. The problem is directly related to the ambiguity inherent in the position of an atomic surface which gives rise to the concept of a Gibbs dividing surface. This ambiguity is discussed in detail in reference 20 and can be resolved by replacing the atomic interfaces by flat Gibbs equimolar interfaces. Employing those methods[20] the following relationships between, s, the length of an edge and, m, the number of Pb atoms on an edge, can be derived for the octahedron, tetrakaidecahedron, and the cuboctahedron.

$$s_{oct} = \left[\sqrt[3]{m_{oct}^3 + \frac{m_{oct}}{2}}\right]\frac{a}{\sqrt{2}} \qquad \text{octahedron}$$

$$s_{tetra} = \left[\sqrt[3]{m_{tetra}^3 - \frac{33m_{tetra}^2}{16} + \frac{3m_{tetra}}{2} - \frac{3}{8}}\right]\frac{a}{\sqrt{2}} \qquad \text{tetrakaidecaheron}$$

$$s_{cub} = \left[\sqrt[3]{m_{cub}^3 - \frac{3m_{cub}^2}{2} + \frac{11m_{cub}}{10} - \frac{3}{10}}\right]\frac{a}{\sqrt{2}} \qquad \text{cuboctahedron}$$

Using these relationships, the areas A_{100} and A_{111} for these three shapes are calculated as a function of m, and the interfacial energies are determined.

The other energy in our analytical model is the strain energy. In order to calculate this energy, we limit ourselves to the case of homogeneous strain. This means that the shape of the Pb inclusion is identical to the shape of the Al void into which it is inserted. Using isotropic elasticity theory and making the approximation that the elastic constants of the two materials are identical, the calculation of the strain energy is straightforward[25]: The strain energy can be written as $E_{strain} = \frac{Ya_{Pb}^3\eta^2}{4(1-\nu)}N_{Pb}$ where Y is Young's modulus, ν is Poisson's

ratio, and η is the strain for the inclusion. The strain is calculated as $\eta = 1 - \left(\frac{N_{Pb}}{N_{Al}}\right)^{1/3} \frac{a_{Pb}}{a_{Al}}$.

For the quantitative calculations, we used the elastic constants for aluminum, Y= 0.39eV/Å^2 and ν=0.35.

In figure 7b, the result of this analytical model is plotted for a number of the smallest polyhedra, allowing direct comparison with the EAM calculations. We deliberately chose shapes with very different aspect ratios and thus very different lengths of the two types of edges. For an octahedron C/A=1.73, for a regular truncated octahedron C/A=1.16, and for a cuboctahedron C/A=0.86. Figure 7a and 7b, are in excellent agreement, especially as regards the relative energies of the three different shapes. Given that the analytical model and the EAM calculations agree at the smallest sizes where edge energies would be most important, it appears that edge energy effects are not responsible for the size-dependent behavior of experimentally measured shapes in Figure 6, in particular the slight increase of the mean and the significant increase in the scatter of the aspect ratio at the smaller sizes. Since edge energy is not responsible for these effects, and they cannot be explained solely by interface energies (as in the Wulff construction), we turn our attention to strain energy, the only remaining possibility. Here we consider how to construct a set of possible precipitate shapes having zero (or very small homogeneous) strain.

We start by observing that an fcc lattice can be built using two fundamental building blocks, a square pyramid (with one atom at each vertex) and a tetrahedron (also with one atom at each vertex). The rhombohedral primitive unit cell of the fcc lattice has one octahedral interstitial site and two tetrahedral interstitial sites. This primitive unit cell is constructed by placing two square pyramids base to base, forming an octahedron, and adding two tetrahedra placed on opposing triangular faces of this octahedron. If one wants to build strain-free fcc Pb precipitate nanoclusters, it can only be done by assembling tetrahedral and square pyramid building blocks having 9 atoms on an edge. Such nanoclusters can be placed in a void created by removing the same Al shape having 11 atoms on an edge. In order to build these shapes with zero strain, the edge length of the tetrahedra and the square pyramids must be 9 times the Pb nearest neighbor distance or 31.5Å. The concept of magic-sizes, discussed

in the literature[22], can be replaced by the criteria of magic-shapes built from tetrahedra and square pyramids with edge length, s_{bb}=31.5Å. For any shape constructed of these building blocks, the strain energy is zero, and the interfacial energy can be calculated based on the interfacial areas, A_{111} and A_{100}, of the shape assembled from these building blocks.

In reality, we are interested not only in completely strain-free precipitates, but also in precipitates having very small homogeneous strains. Examples of such precipitates are listed in table 1 in the columns labeled "tensile strain" and "compressive strain". In order to generate cases such as (m,n) = (4,5), (5,6), (13,16), or (14,17) we approximate them by working with smaller structural building blocks having s_{bb}=15.75Å. (The shapes with zero strain discussed in the previous paragraph can also be assembled from these smaller building blocks). The "magic-shapes" are the set of possible precipitate shapes (and sizes) with zero or small strain built with these building blocks with edge length s_{bb}=15.75Å.

We now have in hand the tools we need in order to explain the experimental data. In particular we have an algorithm to generate a set of precipitates with zero or small homogeneous strain. To illustrate, we will consider precipitates with O_h symmetry, with shapes including the octahedron, and a range of symmetrically truncated octahedra, including the tetrakaidecahedron, the cuboctahedron, and intermediate cases. These precipitates can be formed by starting with an octahedron with edge length s, and removing 6 square pyramids with edge length t. In order that the precipitates be nearly strain-free, the concept of magic-shapes requires that s must be quantized in units of s_{bb}=15.75Å, i.e. s=p s_{bb} where p is a positive integer. Similarly, t must be quantized as t=q s_{bb}, where q is an integer $0 \le q < p/2$.

Since these precipitates are nearly strain-free, and since we have shown that edge energies make only a negligible contribution, the precipitate energies are approximately equal to the interface energies, $E_{precipitate} \approx E_{interface} = A_{111}\gamma_{111} + A_{100}\gamma_{100}$. The aspect ratio is $C/A = (1 - t/s)\sqrt[3]{3}$, the total (100) area is $A_{100}=6t^2$, and the total (111) area is $A_{111}=8s^2-24t^2$. Here we use the T=400K interfacial free energies in order to predict the C/A ratio in agreement with experiment.

At this point, we know the aspect ratio and the approximate energy of all the (nearly) stain-free precipitates with O_h symmetry. In order to predict the observed aspect ratios as a function of precipitate size, we need a criterion for deciding which precipitate energies might actually occur in a quasi-equilibrium distribution of precipitates. For a given precipitate volume, it is easy to calculate the interfacial energy, E_{Wulff}, of a precipitate with the Wulff shape. Since this is the lowest possible energy for a given volume, we find it convenient to work with the energy, $\Delta E = E_{precipitate} - E_{Wulff}$. For precipitates near equilibrium, one would expect a Boltzmann distribution of precipitate shapes with a characteristic $e^{-\Delta E/kT}$ probability. In this experiment, the precipitates are not at equilibrium and one would expect Oswald ripening to continue slowly during further annealing. In order to reproduce the experimental shape distribution (shown as red points in fig. 6), we rejected all precipitate sizes and shapes having $\Delta E > 60eV$. While not rigorous, it appears that this energy criterion allows a shape distribution which, while far from equilibrium, is slowly ripening at the annealing temperature thereby avoiding shapes with very large ΔE. In figure 6 the black symbols represent the complete set of precipitate particles meeting four conditions: O_h symmetry, magic-shape (i.e. near zero strain), $\Delta E \leq 60eV$, and $\overline{A} \leq 55\text{Å}$. The agreement between this "magic-shape" theory and the experimental data is very good.

Finally we note that in addition to the precipitates with O_h symmetry, there are many precipitates which break this symmetry. In all cases, the experimentally observed shapes are consistent with the concept of "magic-shapes" and nearly zero-strain. The inserts in figure 1 shows two such cases. In one insert the symmetry is broken because $A_1 \neq A_2$, while in the other insert, the symmetry is broken by removing a row of tetrahedra and square pyramids to form a notch at an edge along the viewing direction.

To summarize, we have used the embedded atom method in comparison with an analytical calculation of interface and strain energy to conclude that edge energies play a negligible role in determining the shapes of Pb precipitates in Al. Instead we explain the experimental data by assembling "magic-shapes" from building blocks which are tetrahedra and square pyramids with edge lengths, $s_{bb}=15.75$. Given a set of "magic shapes", we find that the

members of this set with relatively small interface energies are the shapes that are observed. This theory provides agreement with many aspects of the experimental data that are otherwise difficult to explain.

References

[1] Nelson, J. Philosophical Magazine A **81**, 2337-2373 (2001).
[2] Nien, C.H. and Madey, T.E., Surf. Sci. **380**, L527 (1997).
[3] O.E. Shklyaev et. al., Phys. Rev. Lett. **94**, 176102 (2005).
[4] E. Johnson et. al., Mat. Sci. and Eng. A **304-306**, 187 (2001)
[5] L. D. Marks, Surf. Sci. **150**, 358 (1985).
[6] S.W. Wang, L.M. Falicov and A.W. Searcy, Surf. Sci. **143**, 609 (1984).
[7] M. J. Kelley, Scripta Met. et Mat. **33**, 1493 (1995).
[8] V. S. Stepanyuk et. al. Phys. Rev. B **62**, 15398 (2000).
[9] B. Voightländer, M. Kästner, and P. Smilauer, Phys. Rev. Lett. **81**, 858 (1998).
[10] I. Daruka, J. Tersoff, and A.-L. Barabási, Phys. Rev. Lett. **82**, 2753 (1999).
[11] N. Moll, M. Scheffler, and E. Pehlke, Phys. Rev. B **58**, 4566 (1998).
[12] A. A. Stekolnikov and F. Bechstedt, Phys. Rev. B **72**, 12536 (2005).
[13] J. W. Gibbs, Collected Works Vol. 1, Longmans, Green and Co., New York 1931, p. 219.
[14] J.S. Rowlinson and B. Widom, "Molecular Theory of Capillarity" Oxford Scientific Publications, 1982, p. 31.
[15] Reference 13, p. 288.
[16] J. Nelson, Philos. Mag. A **81**, 2337 (2001).
[17] C.H. Nien and T.E. Mady, Surf. Sci. **380**, L527 (1997).
[18] O.E. Shklyaev, M.J. Beck, M. Asta, M.J. Miksis, and P.W. Voorhees, Phys. Rev. Lett. **94**, 176102 (2005).
[19] E. Johnson, A. Johansen, U. Dahmen, S. Chen, and T. Fujii, Mater. Sci. Eng. A **304-306**, 187 (2001).
[20] J.C. Hamilton, Phys. Rev. B **73**,125447 (2006).
[21] C.M. Retford, M. Asta, M.J. Miksis, P.W. Voorhees, and E. B. Webb, to be published.
[22] U. Dahmen, S.Q. Xiao, S. Paciornik, E. Johnson and A. Johansen, Phys. Rev. Lett. **78**, 471 (1997).
[23] A. Landa, P. Wynblatt, E. Johnson and U. Dahmen, Acta. Mater. **48**, 2557 (2000).
[24] A. Landa, P. Wynblatt, D.J. Siegel, J.B. Adams, O.N. Mryasov and X.Y. Liu, Acta. Mater. **48**, 1753 (2000).
[25] Khachaturyan, "Theory of Structural Transformations in Solids", John Wiley and Sons, (1983) Chapter 7.

Distribution List

1	MS 9042	Tony Chen	08776
1	MS 9042	Mike Chiesa	08774
1	MS 9161	Sarah Allendorf	08756
1	MS 9161	Art Pontau	08750
1	MS 9292	Blake Simmons	08755
1	MS 9402	Rion Causey	08758
1	MS 9402	John Goldsmith	08772
1	MS 9402	Jean Lee	08759
1	MS 9403	Timothy Shepodd	08778
1	MS 9405	Bob Carling	08700
1	MS 9409	Chris Moen	08757
2	MS 9018	Central Technical Files	8944
2	MS 0899	Technical Library	4536
1	MS 0123	D. Chavez, LDRD Office	1011